Method for estimating dynamic EM tracking accuracy of Surgical Navigation tools

Christopher Nafis[a], Vern Jensen[b], Lee Beauregard[c], Peter Anderson[c]
[a]GE Global Research, 1 Research Circle, Niskayuna NY 12309
[b]GE Healthcare, 384 Wright Brothers Drive, Salt Lake City UT 84116-2862
[c]GE Healthcare, 439 South Union Street, 3rd Floor, Lawrence, MA 01843

ABSTRACT

Optical tracking systems have been used for several years in image guided medical procedures. Vendors often state static accuracies of a single retro-reflective sphere or LED. Expensive coordinate measurement machines (CMM) are used to validate the positional accuracy over the specified working volume. Users are interested in the dynamic accuracy of their tools. The configuration of individual sensors into a unique tool, the calibration of the tool tip, and the motion of the tool contribute additional errors. Electromagnetic (EM) tracking systems are considered an enabling technology for many image guided procedures because they are not limited by line-of-sight restrictions, take minimum space in the operating room, and the sensors can be very small. It is often difficult to quantify the accuracy of EM trackers because they can be affected by field distortion from certain metal objects. Many high-accuracy measurement devices can affect the EM measurements being validated. EM Tracker accuracy tends to vary over the working volume and orientation of the sensors. We present several simple methods for estimating the dynamic accuracy of EM tracked tools. We discuss the characteristics of the EM Tracker used in the GE Healthcare family of surgical navigation systems. Results for other tracking systems are included.

Keywords: Dynamic accuracy, Electromagnetic tracker, Surgical Navigation, Metal Distortion Detection

1. INTRODUCTION

1.1. Motivation

In the image guided surgery arena, a common tracking approach is to use an optical system where line-of-sight requirements limit their practical use for some clinical applications. The size of tools and reference frames, and the amount of space that the equipment takes up in the operating room can disrupt the normal workflow. Tracker vendors are addressing these concerns by making smaller optical sensors and by introducing EM systems.
EM opens up new applications because of the small size of the sensors and their ability to work within objects. Since EM systems operate differently than optical systems, we want to explore their performance and properties. Historically, complaints about EM trackers have been directed primarily at their accuracy and their ability to work around metal equipment and tools.

Vendors often quote tracker system performance in static accuracy as a root-mean-square error (RMS). The method to determine accuracy varies between vendors and products. Static accuracy numbers do not always reflect what the end-users see with their image-guided tools. The new generation of optical trackers quote a single marker static accuracy of 0.25mm (RMS). Previous papers[2,5] suggest that computer-assisted surgery applications desire total system accuracies of 1.5mm or better. The difference between the tracker accuracy and the total system accuracy in an application is outside the scope of this paper. Instead, this paper discusses some simple, cost effective tests that we have found useful to better understand EM (and other) tracker technologies. Our goal for end-users is to present some approaches that will help determine if a particular technology is appropriate for their application. For vendors, we hope these tests will identify areas for tracker improvement.

[a] nafis@crd.ge.com; phone 1 518 387-7167

1.2. EM History

Polhemus invented an AC magnetic field tracking technique for determining the position and orientation of a fighter pilot helmet[16,24]. It used the magnetic field coupling from three orthogonal transmitter coils to three orthogonal sensor coils. A second technique was developed by Ascension Technology that used quasi-DC magnetic fields and fluxgate magnetometers[4]. More recently the focus has shifted to using extremely small sensor coils and an array of transmitter coils.

Electromagnetic navigation has been an important component in image guided surgical systems since 1996. Fried[11] reported results of a multi-center clinical study using the electromagnetic-based InstaTrak® system, concluding the system was accurate and easy to implement during image-guided endoscopic sinus surgery. Others have also confirmed its clinical benefits for sinus surgery[25]. More recently, the use of electromagnetic navigation has been incorporated into image-guided spine surgery[26,27] for lumbar and thoracic pedicle screw placement. It has been used for laporoscopic ultrasonography[6], ultrasound freehand tracking[17,8] and ultrasound bone registration.

There are three commercial companies that sell EM Trackers: NDI[20], Ascension Technology Corporation[1], and Polhemus[23]. There are also several companies that have developed EM trackers as part of their products: Medtronic[19] (AxiEM™), J&J Biosense Webster[3] (CARTO™ XP EP), and GE Healthcare[12] (InstaTrak)

1.3. Application Needs

Minimally invasive clinical applications continue to drive the need for more versatile, accurate, and robust tracking systems. Tracking system position and orientation errors, latencies, and filtering create navigation inaccuracies when coupled with other systems. These tracker issues would be very noticeable in multi-point surface registration methods (Accumatch™), and in applications where 2D imaging systems utilize tracking sensors to build 3D volumes (FluoroCat™ and Tru3D™).

Small EM sensors continue to enable more sub-dermal applications and the tracking of non-rigid devices where sensors can be placed at the distal tip. Tracking metal or conductive tools in any environment with known error tolerances will open up new applications.

1.4. Previous accuracy evaluations

Previous tests have used robotic arms or repeatable fixtures. Some have relied on optical systems with a higher stated accuracy as the reference standard. Others have used a CMM that is traceable to national standards to check their artifacts.

Frantz[10] describes three different protocols for EM accuracy assessment. The first uses a 3-axis robot with a non-metallic end effector that can be rotated. It appears that the "true" position is determined by an NDI Optotrak™ system that quotes 0.15mm accuracies. EM sensors are mounted at different orientations on the end of the arm. The second protocol uses a known hemispherical artifact that was checked with a CMM. A sensor probe is checked against 50 radially-directed holes. The last protocol uses a ceramic ball bar that has two sensors attached to it. The sensors are characterized so their origins are centered in the balls. The ball bar is moved randomly around the working volume in different orientations. The reported 3D distances between the sensors are compared to the true value for accuracy, and the standard deviation is used for the precision. Frantz uses the ball bar data as a nice example of the inherent problems of data reduction.

Schicho[28] evaluated the Medtronic Treon™ EM and NDI Aurora® systems in simulated operating room conditions using a large Langenbeck hook, a dental drill with its handle and an ultrasonic scanhead. They concluded that the Medtronic StealthStation™ Treon EM and the NDI Aurora showed stable performance in the presence of the surgical instruments. They recommended mandatory accuracy security margins be set and that simple stability tests be done on all surgical instruments.

Hummel[13] tested an Aurora system and introduced closed metallic loops, wire guides, catheters, ultrasound probes, and c-arms. He found that the tracker was shown to be more sensitive to distortions caused by materials near the EM field emitter. Distortions caused by materials near the sensor were smaller. The C-arm unit caused considerable distortions

and limited the reliability of the tracker. Metal distortion was tested by mounting an EM field transmitter and a sensor at a fixed distance from each other. A distorter was then moved to different repeatable locations between the two. The data from the undistorted and the distorted datasets were used to calculate the distortion error.

Hummel[14] compared the Ascension microBIRD™ and NDI Aurora using a precision machined plate with holes to measure position and orientation accuracy. They mounted an optical sensor at a fixed distance from the EM sensor and moved the pair randomly around the working volume to understand dynamic behavior. Finally they measured the distortion caused by metallic objects by inserting metal rods at various locations around the working volume. There is no mention of traceability to a standard, although a CMM should be able to validate the machined base plate. In the past we have noticed repeatability problems with blocks and pegs because of dirt and wear. In the dynamic test a NDI Polaris™ optical sensor was used as a reference. The quoted static accuracy of the Polaris is 0.35mm and not that different from the Aurora. A higher accuracy device like the NDI Optotrak should be used.

2. MATERIALS AND METHODS

We used a NIST certified granite block and a robot with a large composite arm that was calibrated by a NIST traceable Laser Tracking Interferometer for the tests. Two tests were done to validate the vendor's quoted static accuracy. Three tests were done to look at dynamic precision and accuracy. A final test was done to determine the effects of different metals on the dynamic tracking and accuracy.
Our aim was to create simple, fast tests that could be done with inexpensive, easily obtainable objects that were traceable to a national standard. We wanted to look at dynamic behavior and collect large datasets to understand the distributions. The assumption was that the data would not be normal. We assumed that the EM trackers would be affected by metal distortion. We were interested to see if the trackers could dynamically detect the distortion and limit the bad data used by the surgical navigation systems. We wanted tests that would lend themselves to tracked tools and catheters, not just raw sensors. Test portability and duration are of some concern, since the opportunity to test equipment is often at trade-shows or visits to the vendor.

2.1. Static Precision

The EM field transmitter and receiver were placed on a flat surface 12 inches (304.8mm) apart (Figure 1). The measurement environment was EM friendly (no metal or conductive materials nearby). 1000 measurements were taken. The standard deviation, 95th percentile from the distance mean, and span (maximum distance – minimum distance reported) were calculated. Though this test could easily be repeated at different distances, twelve inches was chosen so a broad range of trackers could be compared. The distributions typically broaden as the distance between the transmitter and receiver increases. Span usually increases with the number of samples, but is still interesting to compare.

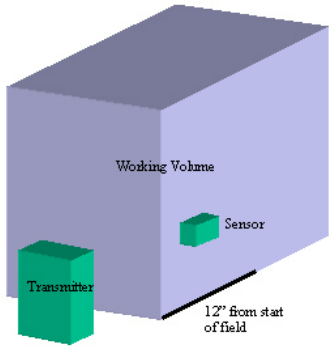

Figure 1. Static precision setup

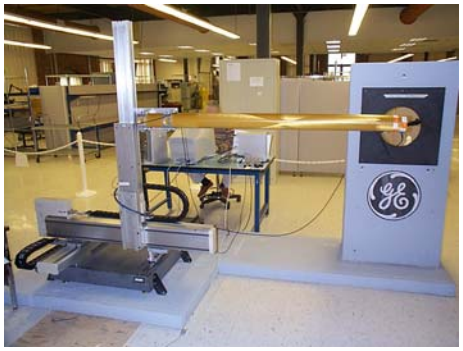

Figure 2. Static accuracy 3-axis robot

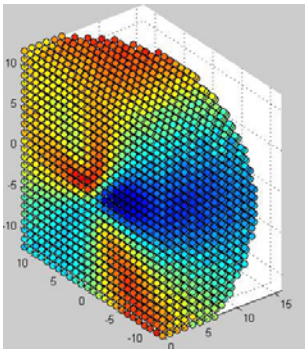

Figure 3. Robot static accuracy color error map

2.2. Static Accuracy

A 3-axis robot with a composite arm (Figure 2) was used to collect data on a one inch grid throughout a tracker's working volume (up to a 24x24x24 inch volume). The arm position was validated with a NIST traceable Laser Tracking Interferometer[7] (3D single point accuracy @ 2m of 0.033mm). The tools or sensors were mounted on the robot arm. Thirty samples were taken at each location and averaged. The resulting point cloud and the robot coordinate system were then aligned. The standard deviation, RMS, 95th percentile, and maximum error were calculated between the robot coordinates and the tracker coordinates for each point on the grid. Visualization techniques such as cut planes, color difference maps, and animation were found to be useful in trying to understand the underlying EM field (Figure 3).

2.3. Dynamic Precision at different speeds

For systems that support two or more sensors, two sensors were placed a fixed distance apart on a rigid board. The board containing the two sensors was moved in a random spiral pattern throughout the working volume (Figure 4). The spirals were done in different orientations. Each data sample was time-stamped and an average velocity (mm/sec.) was calculated. 1000 samples were collected, and for each sample the distance between the sensors was calculated. The standard deviation, 95th percentile, and the span were calculated for each experiment. The experiment was repeated at different velocities.

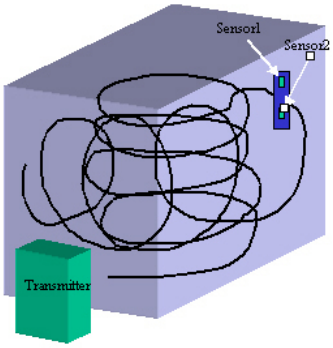

Figure 4. Dynamic distance setup

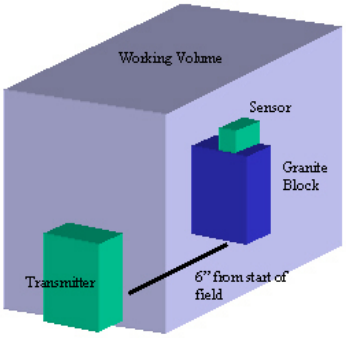

Figure 5. Dynamic precision setup

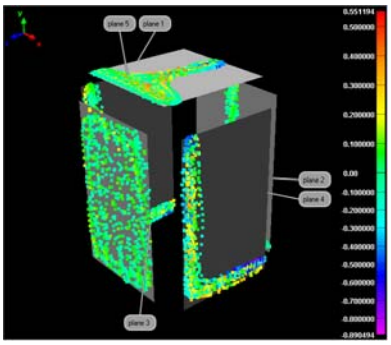

Figure 6. Color error displacement map of plane fit

2.4. Dynamic Precision

A precision NIST traceable 6x6x9" granite block[30] that has 6 finished faces that are flat, square, and parallel to 0.00005" per 6" was used. The front face of the block was placed 6 inches from the EM Transmitter (Figure 5). Initial experiments with the Polhemus Fastrak™ showed performance degraded as the block was moved further from the transmitter (Figure 21). The six inch distance was chosen so a variety of sensors could be compared. A raw sensor or calibrated tool tip was "scribbled" on the five accessible surfaces. By "scribbling", we mean moving the sensor randomly over a precision flat surface of the granite block and collecting points as we move the sensor. Thousands of points were collected on each face. The sensor was held in four different 90° orientations for each face (Figure 7). The collected points were best-fit to planes. Each point was then compared to the plane to calculate a standard deviation, RMS, maximum error, 95th percentile, and span. The data can be visualized with color difference maps (Figure 6) that show the point cloud deviation from the planes using software like Innovmetric Polyworks®[15].

Figure 7. Raw sensor scribbling orientations

If the tracking system only had one sensor, the granite block and the transmitter were attached to the test surface. Systems with two sensors allowed one of the sensors to be attached to the granite block as a coordinate system reference. In these cases, the sensor being measured is in the coordinate system of the other sensor, which is also being measured and hence subject to measurement error. We would expect the overall errors in these cases to be slightly higher than they would be if only a single sensor was used. Very small sensors that didn't have a smooth surface, or tools (e.g. catheters, needles), were affixed to small plastic blocks (Figure 8, Figure 9). This allowed them to easily be "scribbled" on the granite block.

Figure 8. Microsensor attached to plastic

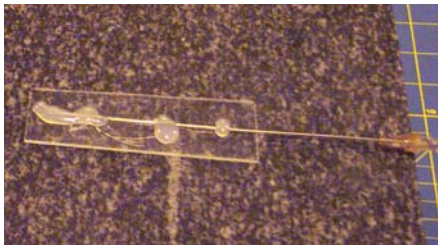

Figure 9. 5DOF needle attached to plastic

2.5. Dynamic Accuracy

For tools such as pointers that have calibrated tips, the accuracy can be determined by "scribbling" at least five sides of the granite block. The pointer is held in four different 90° orientations for each face (Figure 10). Thousands of points are taken and the resulting point cloud is best-fit to a CAD model of the granite block using Polyworks IMInspector™[15]. The mean, standard deviation, RMS, maximum error, maximum 95th percentile, and span are calculated between each point in the cloud and its closest point on the CAD model surface. For pointers with ball tips, the radius has to be taken into consideration when comparing to the CAD model.

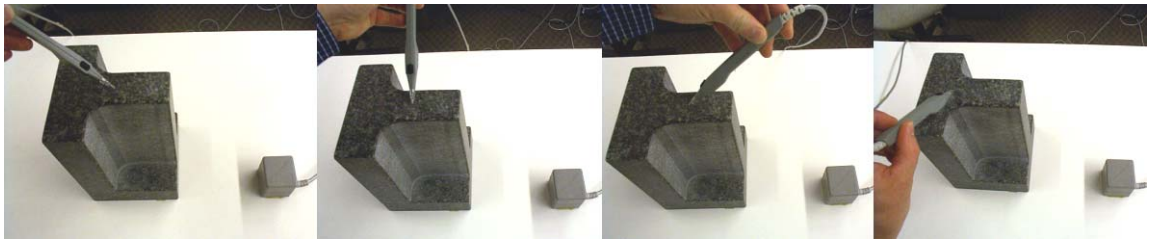

Figure 10. Probe orientations for scribbling

When sensors or tools are glued to a piece of plastic, the granite block can be used to calibrate the sensor offset. Although you lose an independent way to check accuracy, you can still fit the adjusted point cloud to the CAD model of the block. This will help show any distortion in the data.

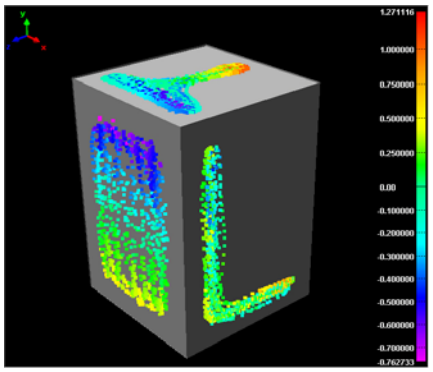

Figure 11. Color error displacement map of CAD alignment

2.6. Dynamic Metal Distortion Detection

We were interested in how well the EM trackers worked around metal distorters. Ideally, they would accurately track in any environment. If they are unable to track, then we would like them to exclude any bad data by dynamically detecting the distortion. The precision granite block is used again. First data is "scribbled" on one or more planes without any distorters present. The sensor orientation is varied during the data collection process. This data is best-fit to one or more planes and constitutes our base-line. Different metal objects are then placed between the EM field transmitter and the granite block (Figure 12). Data is then re-collected by "scribbling" on the granite block with the distorter present. This point cloud is then compared to the reference plane(s). Only data that was considered "undistorted" by the tracker is used.

Seven different distorters were tested (17-4, 304, 440C, Nitronic stainless steel, titanium, ferrous metal spray paint can, and an aluminum soda can). The percentage of undistorted points returned, mean, standard deviation, RMS, 95th percentile, maximum error, and percentage of trackable area were calculated. The trackable area was determined by placing a 1 inch grid on the data and scoring areas that contained data.

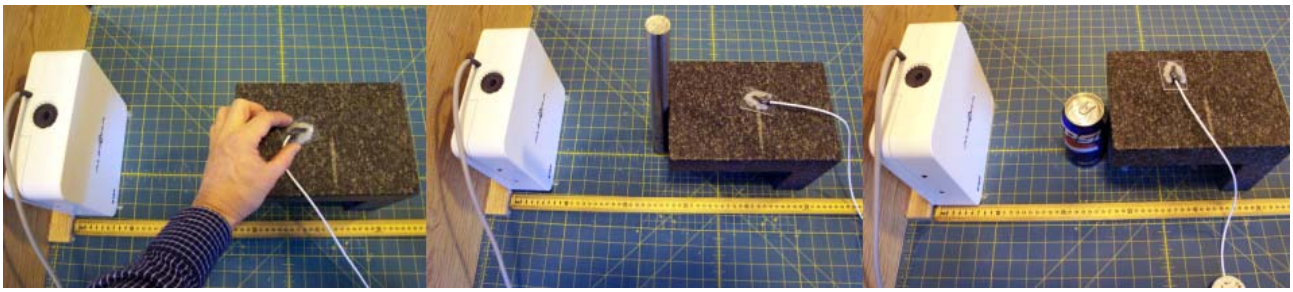

Figure 12. Collecting non-distorted and distorted data

3. RESULTS

3.1. Vendor Stated Accuracies

Vendors have different ways of specifying accuracy, but always quote static accuracy.

3.1.1. Ascension microBIRD™

Ascension states a static accuracy of 1.4mm RMS and Orientation of 0.5 degree at 30.5cm. For Model 130: the accuracy test volume was X from 20cm to 36cm, Y&Z from –15cm to 15cm. For Model 180: the accuracy test volume was X from 20cm to 51cm, Y&Z from –23cm to +23cm. The EM transmitter is a 9.6cm cube and the 6DOF sensor has a 1.8mm diameter. The update rate is 90Hz.

3.1.2. Ascension pciBIRD™

Ascension states a static accuracy of 1.0mm RMS and 0.5 degrees RMS over the range from 20.3 cm to 76.2cm. The EM transmitter is a 9.6cm cube and the 6DOF sensor is 25x25x20mm. The update rate is 105Hz.

3.1.3. Ascension Flock of Birds Class B®

Ascension states a static accuracy of 1.8mm RMS and 0.5 degrees RMS over the range from 20.3 cm to 76.2cm. The EM transmitter is a 9.6cm cube and the 6DOF sensor is 25.4x 25.4mx 20.3mm. The update rate is 144Hz.

3.1.4. GE InstaTrak® Gold

The EM tracker internal to the GE InstaTrak system is an alternating current (AC) system. It has a small three orthogonal coil transmitter that can be attached to an Ears-Nose-Throat (ENT) headset or a bone pin. The receiver is made to repeatably snap into different tools. The receiver contains a pair of three orthogonal coil sensors. With the pin transmitter, the receiver works in a 36 inch (91.4cm) sphere centered around the transmitter. The small transmitter size allows it to be used right in the area of interest. The EM transmitter is 15x17x70mm and the snap packs receivers are 16x17x67mm. The update rate is 34Hz for four sensors.

3.1.5. NDI Aurora® EM Tracker

NDI Aurora quotes accuracy differently for 5DOF and 6DOF tools. The Aurora working volume is 500x500x500mm. The maximum measurement rate with 5 or less sensor coils is 40Hz. With 6 or more sensor coils the update rate is 20Hz. The EM Field generator is 200x200x70mm and the individual coils have a 0.8mm diameter.

NDI Aurora 5DOF accuracy is based on more than 300 random positions and orientations distributed throughout the sub-volume

Position

Radial distance from Field Generator (mm)	*RMS*	*95% confidence Level*
100-200	0.9mm	1.7mm
200-300	0.7mm	1.3mm
300-400	0.8mm	1.4mm
400-500	1.3mm	2.1mm

Orientation

Entire Volume	0.3degrees	0.6 degrees

NDI Aurora 6DOF accuracy is based on a calibrated artifact consisting of more than 40 predetermined random positions and orientations distributed over a 150mm diameter hemisphere.

Position

Artifact distance from Field Generator (mm)	*RMS*	*95% confidence Level*
250	0.9mm	2.0mm
450	1.6mm	3.0mm

Orientation

250	0.8 degrees	1.5 degrees
450	1.1 degrees	1.7 degrees

3.1.6. NDI Vicra™ Optical Tracker

NDI Vicra™ quotes an accuracy (0.25mm RMS) of a single marker stepped through more than 500 positions throughout the measurement volume using the mean of 30 samples at each position at 20º C. The camera offset is 557mm. The working volume is an odd shape. At the beginning of the field it is 491 x 392mm. At the back of the field (1336mm) the field is 938 x 887mm. The maximum update rate is 20Hz.

3.1.7. Polhemus FASTRAK®

Polhemus FASTRAK quotes a static accuracy of 0.03 inches (0.76mm) RMS for the X, Y, or Z positions; 0.15 degrees RMS for receiver orientation. The specified update rate is 120 updates/second divided by the number of receivers. The latency is 4 milliseconds. The standard EM transmitter is 58x56x56mm and the sensor is 23x28x15mm.

3.1.8. Polhemus Liberty™

Polhemus LIBERTY quotes a static accuracy of 0.03 inches (0.76mm) RMS for X, Y, or Z position; 0.15 degrees RMS for sensor orientation in a 36 inch (91.4cm) working volume. The specified update rate is 240Hz per sensor with a 3.5 millisecond latency. The standard EM transmitter is 58x56x56mm and the sensor is 23x28x15mm.

3.2. Static Precision

At first glance, the 1000 samples taken at 12 inches (304.8mm) only tells us that some of the EM trackers have static noise levels similar to that of the benchmark Vicra optical system. This precision test was then expanded to use the robot to test different distances between the transmitter and the sensor as shown in Figure 14. Some systems show different precisions depending on the location in the working volume. The NDI Aurora 5DOF sensor seems to be sensitive to the orientation of the 5DOF coil relative to the EM field transmitter.

Tracker Configuration	Standard Deviation [mm]	95% from mean [mm]	Span [mm]
Ascension pciBIRD	0.03	0.07	0.17
Ascension microBIRD	0.02	0.01*	0.24
Ascension Flock Class B	0.10	0.27	0.50
GE InstaTrak Gold	0.03	0.08	0.14
NDI Aurora 5DOF parallel	0.06	0.12	0.33
NDI Aurora 5DOF towards	0.09	0.17	0.59
NDI Aurora 6DOF	0.03	0.06	0.20
NDI Vicra linear 3 ball probe	0.03	0.05	0.16
Polhemus Fastrak	0.006	0.0003*	0.11

Figure 13 Static Precision Table *note these two systems had non-normal distributions

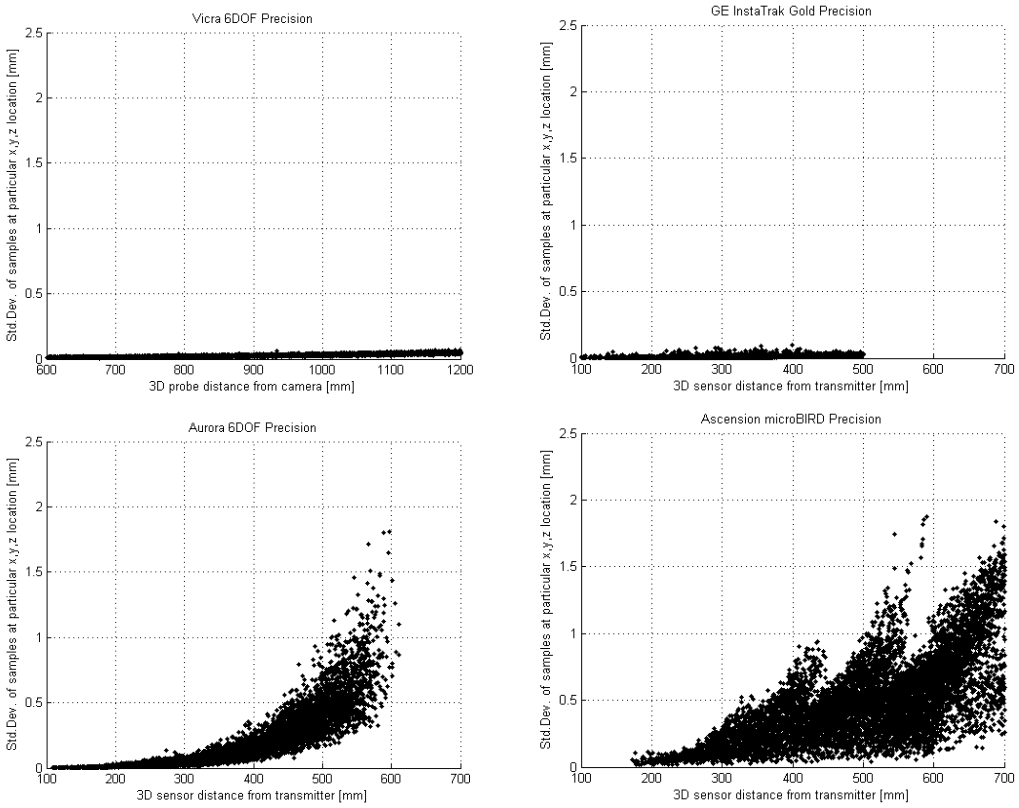

Figure 14. Robot static position precision results

3.3. Static Accuracy

We wanted to validate the static position accuracy of the trackers before moving on to the dynamic tests. For this we used a high accuracy composite robot, which would be inaccessible to most people. Our tests show similar results to the NDI Vicra single marker specification (0.27mm versus 0.25mm RMS). For the NDI Aurora 6DOF our 1.07mm RMS and 2.15mm 95th percentile for the whole working volume were slightly better than the 1.6mm RMS and 3.0mm 95th percentile that NDI reports for the artifact at 450mm. For the Aurora 5DOF our 1.46mm RMS and 2.30mm 95th percentile for the entire working volume was slightly worse than the 1.3mm RMS and 2.1mm 95th percentile reported at 400-500mm radial distances. The 0.90mm RMS we saw with the new Ascension microBIRD external unit tested in a 580x580x580mm working volume was better than the 1.4mm RMS specified in a smaller working volume. It is evident from Figure 14 and Figure 17 that the Aurora / microBIRD precision and accuracy decrease with radial distance. It is also interesting to note the improvement of the current microBIRD from the one tested just 18 months ago.

Tracker Configuration	**Standard Deviation [mm]**	**RMS [mm]**	**95% [mm]**	**Maximum Error [mm]**	**# positions on 1" grid**
Ascension microBIRD PCIcard 1.8mm sensor with cube transmitter (*note only one sample was taken at each position 6/2004)	0.63	1.10	2.09	11.93	5988
Ascension microBIRD external 1.8mm sensor with cube transmitter (12/2005)	0.46	0.90	1.77	3.61	8370
GE InstaTrak Gold receiver snap pack	0.17	0.40	0.67	1.14	8311
NDI Vicra linear 3 ball probe (12/2005)	0.18	0.27	0.49	2.04	5759
NDI Aurora 6DOF Reference (12/2005)	0.61	1.07	2.15	4.56	6422
NDI Aurora 5DOF needle (12/2005)	0.83	1.46	2.30	5.79	6445

Figure 15 Static Accuracy Table

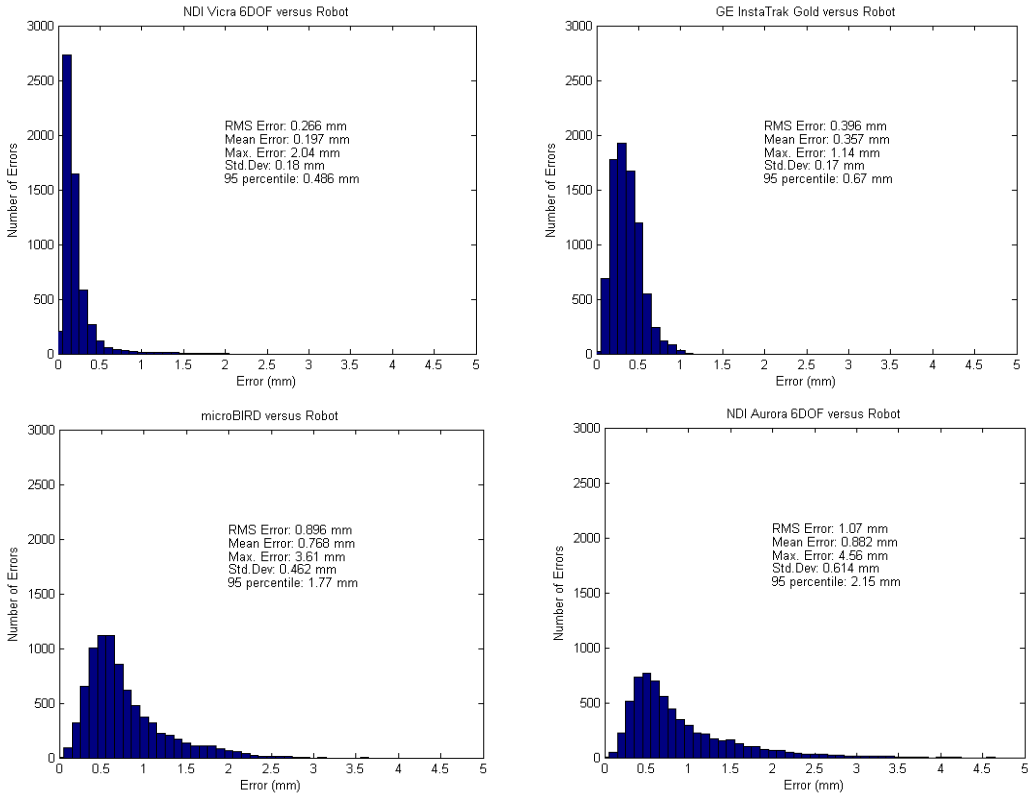

Figure 16. Robot static position accuracy distributions

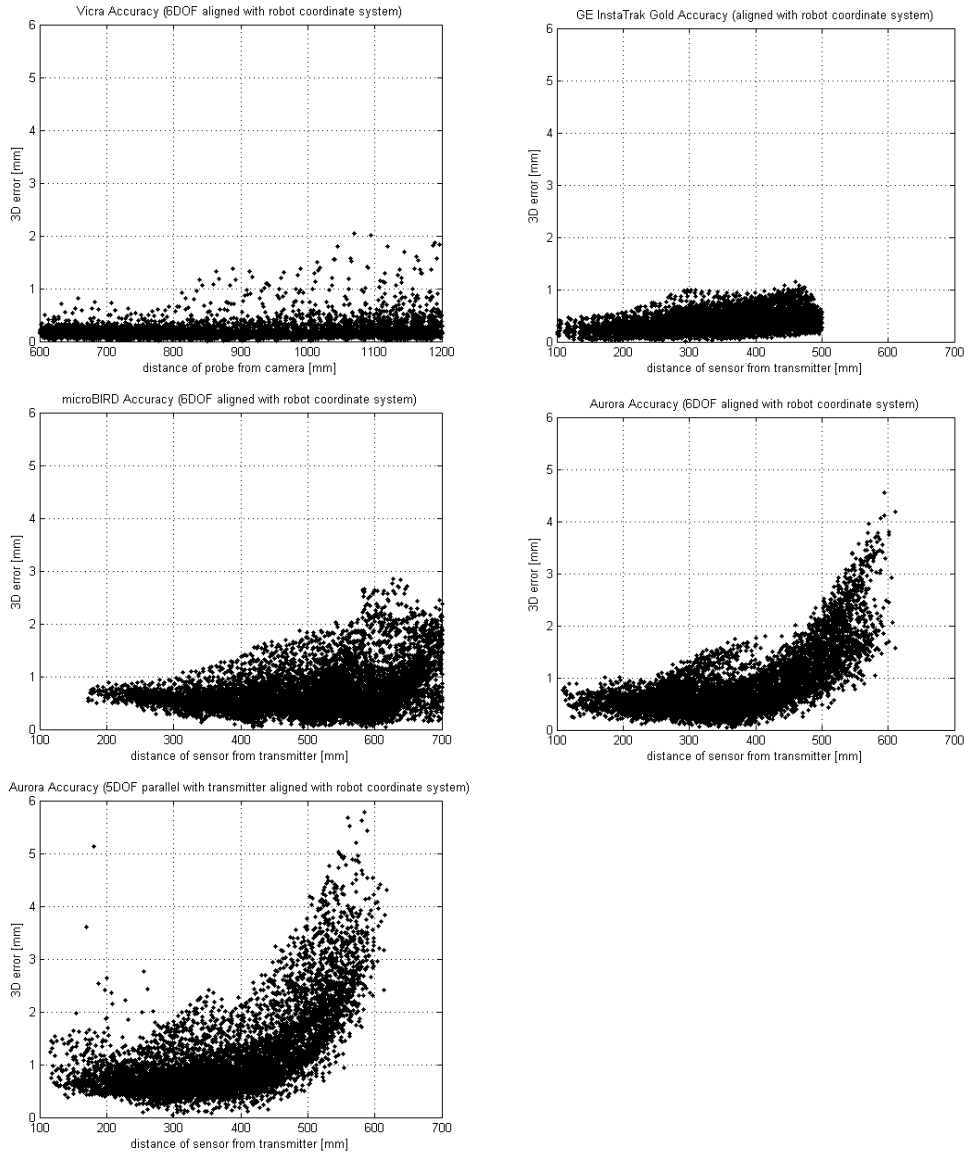

Figure 17. Robot static position accuracy results

3.4. Dynamic Precision

3.4.1. Constant distance

This test is not traceable to a national standard, but it does help understand at what rates tools can be tracked before the errors become unacceptable. Since the two sensors are fixed in relation to each other, their reported 3D separation should not change during motion. Because of sensor position and orientation errors, you get a distribution of reported distances. With certain implementations, the distribution widens with increased motion. The NDI Aurora reported an increased number of “MISSINGS” (where a position / orientation solution could not be calculated) when the tool speed was increased. The NDI Vicra optical system showed no motion issues using two 4-marker references. A test at an average velocity of 467mm/sec. showed the standard deviation was 0.09mm, 95th percentile was 0.17mm, and the span was 0.65mm. Ten percent of the points requested had “too few marker” errors. For many high accuracy applications, movements are fairly slow and speeds of less than 100mm/sec. should be adequate.

Tracker Configuration	Std.Dev. @ 50mm/sec. [mm]	95th % @ 50mm/sec. [mm]	Span @ 50mm/sec. [mm]	Std.Dev. @ 100mm/sec. [mm]	95th % @ 100mm/sec. [mm]	Span @ 100mm/sec. [mm]
Ascension microBIRD	1.12	2.29	14.1	1.34	2.63	18.1
Ascension pciBIRD	1.04	2.17	7.21	1.19	2.56	8.00
GE InstaTrak Gold	0.14	0.27	0.79	0.20	0.38	1.07
NDI Aurora	0.26	0.54	1.83	0.34	0.64	3.11
Polhemus Fastrak	0.58	1.19	2.88	1.15	2.38	5.77

Figure 18. Distance data interpolated at 50 and 100 mm/sec.

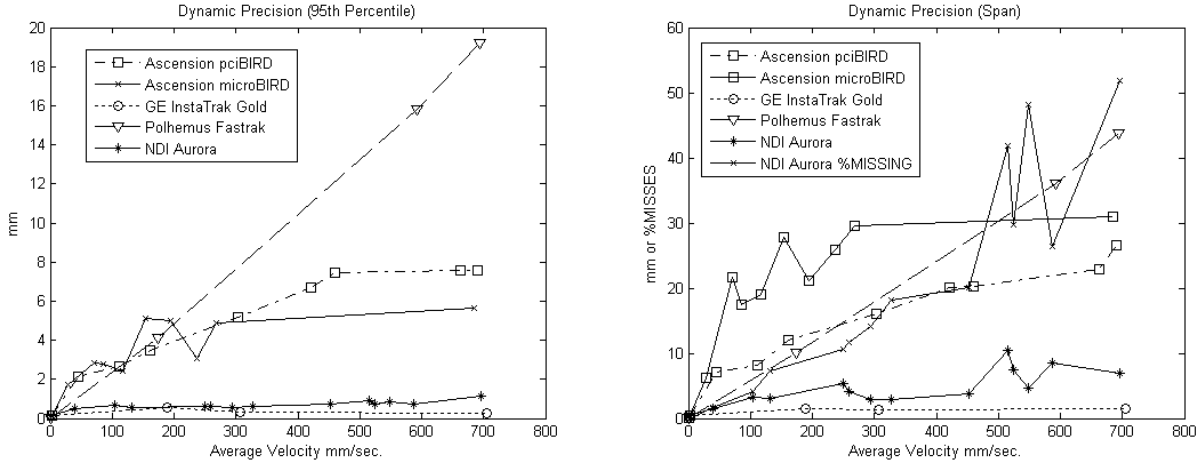

Figure 19 Constant Distance Velocity Graphs

3.4.2. Scribbled block

The new Aurora and microBIRD systems showed very similar results. The low noise and stability of the GE InstaTrak that was evident throughout the working volume in the robot and constant distance tests, was also apparent in this test.

Tracker Configuration	Standard Deviation [mm]	RMS [mm]	95% [mm]	Maximum Error [mm]	Span [mm]
Ascension microBIRD PCI card 1.8mm sensor on plastic block 6 inches from cube transmitter (6/2004)	0.85	0.85	1.89	7.17	11.78
Ascension microBIRD external 1.8mm sensor on plastic block 6 inches from cube transmitter	0.60	0.60	1.36	3.83	6.75
Ascension pciBIRD raw receiver	0.27	0.27	0.56	1.56	3.04
Ascension Class B Flock raw receiver with block 12 inches from transmitter	0.37	0.37	0.76	2.82	4.96
Ascension Class B Flock receiver mounted on 1.5mm ball probe	0.52	0.52	1.09	3.03	4.92
GE InstaTrak Gold 4.7cm pointer with 1.5mm ball tip	0.13	0.13	0.26	0.57	1.11
NDI Vicra linear probe 3mm ruby tip with 3 balls with system reference	0.30	0.30	0.59	1.17	2.27
NDI Vicra probe with 0.8mm tip with 4 balls with system reference	0.22	0.22	0.44	1.14	1.91
NDI Polaris active probe with 3mm ruby tip and system reference	0.16	0.16	0.35	0.64	1.21

NDI Aurora with Traxtal 6DOF MP006 Probe with system reference	0.66	0.66	1.40	4.75	8.01
NDI Aurora with 5DOF needle mounted on plastic with system reference	0.69	0.69	1.34	8.04	15.04
NDI Aurora with 6DOF reference mounted on plastic with system reference	0.57	0.57	1.17	4.74	8.15
Polhemus Fastrak with ST8 Stylus block 6 inches from transmitter	0.10	0.10	0.20	0.51	0.90
Polhemus Fastrak raw receiver with block 6 inches from transmitter	0.13	0.13	0.25	0.51	1.02
Polhemus Fastrak raw receiver with block 12 inches from transmitter	0.16	0.16	0.35	0.89	1.44
Polhemus Fastrak raw receiver with block 18 inches from transmitter	0.44	0.44	0.84	3.53	4.54
Polhemus Fastrak raw receiver with block 24 inches from transmitter	0.51	0.51	1.06	3.00	5.35
Polhemus Liberty prototype raw receiver with block 18 inches from transmitter	0.19	0.20	0.48	0.97	1.71

Figure 20 Dynamic Precision Table

3.5. Dynamic Accuracy

The Polhemus Fastrak data taken with the granite block at different distances show how the system accuracy; standard deviation, RMS, 95th percentile, and span, all degrade with distance. This same effect is seen with other trackers in more detail in the static robot tests. A vast improvement can be seen between the first and second generation of the NDI Aurora system. The NDI Vicra 0.8mm tip probe results show the importance of tool design and tip offset. In this test the Polaris active 4 LED probe was slightly better than the Vicra 3 marker passive linear probe. The GE InstaTrak probe and the Polhemus ST8 probe had better results than the optical systems. Although it should be noted that the ST8 has its EM coils mounted very close to the probe tip. This reduces the lever arm effect of orientation errors.

Tracker Configuration	**Mean [mm]**	**Standard Deviation [mm]**	**RMS [mm]**	**95% [mm]**	**Maximum Error [mm]**	**Span [mm]**
Ascension Class B Flock receiver mounted on 1.5mm ball probe	-0.61	062	0.87	1.56	2.71	4.74
GE InstaTrak Gold Short pointer with 1.5mm ball tip	-0.22	0.16	0.27	0.48	0.90	1.33
NDI Aurora with Traxtal 6DOF MP006 Probe with block 6 inches from Tetrahedral transmitter (12/2003)		2.17			17.09	33.63
NDI Aurora with Traxtal 6DOF MP006 Probe with system reference	-0.39	0.70	0.80	1.58	5.12	7.78
NDI Polaris active probe with 3mm ruby tip and system reference	-0.26	0.30	0.39	0.72	1.24	1.62
NDI Vicra linear probe 3mm ruby tip with 3 balls	0.26	0.46	0.53	0.98	1.56	3.07
NDI Vicra probe with 0.8mm tip with 4 balls	0.79	0.26	0.84	1.25	1.78	2.22
Polhemus Fastrak with ST8 Stylus block 6 inches from transmitter	0.00	0.14	0.14	0.26	0.49	0.96
Polhemus Fastrak raw receiver with block 6 inches from transmitter	0.14	0.14	0.20	0.35	0.53	0.98
Polhemus Fastrak raw receiver with block 12 inches from transmitter	-0.00	0.25	0.25	0.51	0.94	1.70
Polhemus Fastrak raw receiver with block 18 inches from transmitter	0.04	0.59	0.59	1.12	3.22	4.51
Polhemus Fastrak raw receiver with block 24 inches from transmitter	-0.11	1.84	1.84	3.89	9.91	17.22
Polhemus Liberty prototype raw receiver with block 18 inches from transmitter (8/2003)	0.33	0.63	0.71	1.47	2.27	3.13

Figure 21 Dynamic Accuracy Table

3.6. Dynamic Metal Distortion Detection

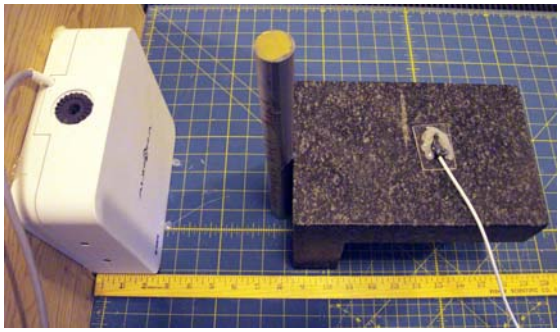

Figure 22. 17-4 Stainless steel distorter placement

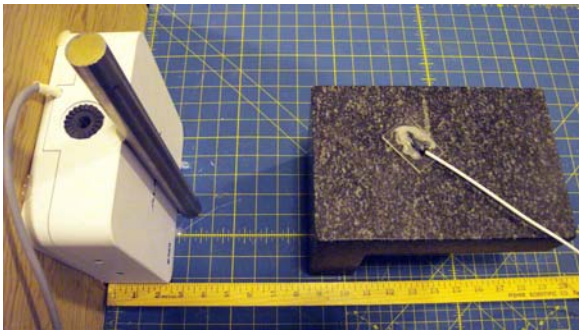

Figure 23. Distorter placed next to EM field transmitter

Several of the EM trackers report a quality indicator along with the position and orientation data. We used these indicators to determine if a point should be used or not.

For example, you can see the effect of using the NDI Aurora quality term from a 6DOF sensor (5DOF sensors don't report quality). The images (Figure 25) show the data collected with the quality term < 1 (as suggested by NDI) versus using all the data (Figure 24). A 17-4 stainless steel rod was used as a distorter. For the data that used the quality term, the maximum error = 4.94 mm. If all the data is used, then the mean of data is 1.26mm, 95th percent of data is within 6.51mm of plane, the plane fit standard deviation = 3.64mm, the RMS = 3.85mm, the maximum error = 27.61mm, and the span = 47.70mm! The trade-off of using the quality term is that data can't be collected in some areas.

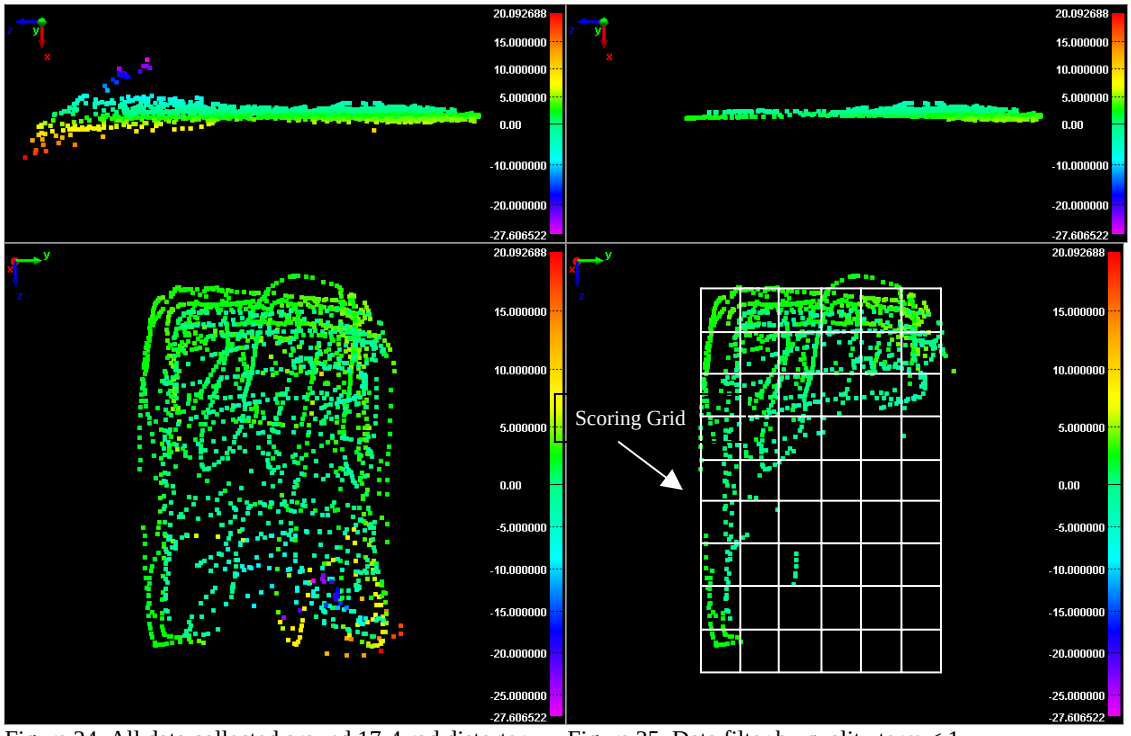

Figure 24. All data collected around 17-4 rod distorter

Figure 25. Data filter by quality term < 1

If the distorter was placed right next to the EM field transmitter (Figure 23), things were not too interesting. Every point was thrown out as having a poor quality number.

The Ascension Class B Flock did not track well around high ferrous content metals. The GE InstaTrak did not track well near the aluminum soda can and the ferrous metal spray paint can. When using the quality indicators, both systems had maximum errors less than 3mm. The NDI Aurora was able to track closer to all the test distorter types, but its maximum errors were higher. The Polhemus Fastrak does not report a quality indicator. The Polhemus Liberty has a distortion alarm that can be triggered by any sensor. We did not have a chance to test this during our plant visit.

Tracker Configuration	**Distorter**	**Percentage of non-distorted points returned**	**Mean [mm]**	**Standard Deviation [mm]**	**RMS [mm]**	**95% [mm]**	**Maximum Error [mm]**	**Span [mm]**	**Trackable Area %**
Ascension Class B Flock raw receiver[a]	None	100%	0.06	0.59	0.60	1.24	1.85	3.40	100%
	Type 17-4 Stainless Steel	0%							0%
	Type 304 Stainless Steel	97%	0.13	0.89	0.90	1.55	2.09	4.13	100%
	Type 440C Stainless Steel	0%							0%
	Nitronic Stainless Steel	98%	0.08	0.94	0.94	1.71	2.34	4.47	100%
	Titanium	100%	0.09	0.92	0.92	1.78	2.24	4.30	100%
	Spray Paint Can	0%							0%
	Aluminum soda can	100%	0.13	0.62	0.63	1.20	1.96	3.22	100%
GE InstaTrak Gold Snap Receiver[b]	None	100%	0.00	0.14	0.14	0.31	0.46	0.92	100%
	Type 17-4 Stainless Steel	90%	0.88	0.29	0.92	1.34	1.78	1.92	96%
	Type 304 Stainless Steel	59%	1.04	0.37	1.10	1.55	2.10	2.91	83%
	Type 440C Stainless Steel	98%	1.75	0.20	1.76	2.06	2.68	1.62	100%
	Nitronic Stainless Steel	53%	0.97	0.34	1.03	1.41	1.64	2.55	85%
	Titanium	69%	0.73	0.35	0.81	1.22	1.73	2.77	85%
	Spray Paint Can	0%							0%
	Aluminum soda can	0%							0%
NDI Aurora with 6DOF reference tool[c]	None	97%	-0.06	0.31	0.32	0.64	3.04	4.86	100%
	Type 17-4 Stainless Steel	42%	1.45	1.85	2.35	4.13	4.94	8.64	54%
	Type 304 Stainless Steel	98%	0.21	0.28	0.35	0.65	1.78	2.87	100%
	Type 440C Stainless Steel	53%	1.53	1.91	2.45	4.04	5.52	8.76	83%
	Nitronic Stainless Steel	99%	0.02	0.34	0.34	0.65	2.46	3.91	100%
	Titanium	98%	0.03	0.28	0.28	0.55	1.65	3.16	100%
	Spray Paint Can	58%	-1.27	1.40	1.89	3.33	4.10	7.43	96%
	Aluminum soda can	98%	0.16	0.42	0.45	0.79	1.52	2.52	100%

Figure 26 Metal Distortion Table

[a] A value of 76 was used as a cutoff threshold. In the tests the maximum value of 127 was always returned
[b] GE InstaTrak returns two quality terms FID and GOF. The cutoff used was GOF < 0.001 and FID < 5
[c] A value of 1 was used as a cutoff threshold

4. DISCUSSION AND CONCLUSION

We have demonstrated several simple, quick, and inexpensive tests to evaluate the dynamic performance of EM tracked tools. These are not exhaustive and should be considered additional techniques in the analysis toolbox. The granite block scribbling test provides a good indication of the results that someone would see using a tool to collect registration points. Our results show that depending on the implementation, EM trackers can attain dynamic precision and accuracy results similar to those of the new generation of small optical trackers. It also shows that EM trackers can be affected by metal distortion. Although the EM tracking systems may not always be able to track in metal distorted environments, they can usually detect the distortion and limit the number of bad points passed on to the application. Our tests show that significant progress has been made in EM tracking in the past year or two. The latest generation of EM Trackers continue to improve their receiver size, accuracy, and metal tolerance.

It was difficult to compare our results to previous studies because of rapidly changing tracker systems and the special artifacts used. We initially only intended to share the procedures that we have found helpful. As vendors provided us their latest equipment, it provided an opportunity to highlight the performance of the latest generation of optical and EM trackers.

There are several limitations to our study. Our tests show the precision and accuracy of the trackers only. They do not show the overall performance of the complete navigation system. We looked at different metal distorters, but did not use common tools specific to the surgical operating room. Our tests were completed primarily by a single operator over a period of several years. The tests were run on systems with different design attributes. It may not make sense to directly compare them. We used the default parameters for every tracker. Some trackers (e.g. Ascension) can be optimized for the specific environments.

We hope others will use these tests and publish their tracker system results, and that a standard set of tests emerge that the entire community can embrace.

ACKNOWLEDGMENTS

Northern Digital, Inc. supplied us with their new Vicra optical tracker and Aurora EM systems for evaluation. Special thanks to Jeff Stanley, Stefan Kirsch, and Saibal Chakraburtty for all their help and direction. Ascension Technology Corporation supplied their pciBIRD, microBIRD, and Flock of Birds Class B for evaluation. Special thanks to Trish Scott and Mark Schneider for their support and suggestions. Lisa Last and Alex Li were very generous with access and many hours on their 3-axis robot. They helped collect data and provided MATLAB® algorithms to process the data. Vianney Battle, Donna Fairbanks, Mark Grabb, and Cindy Landberg provided encouragement and support in preparation of this paper.

REFERENCES

1. Ascension Technology Corporation, http://www.ascension-tech.com/
2. Birkfellner W, Watzinger F, Wanschitz F, Ewers R, Bergmann H, “Calibration of tracking systems in a surgical environment”, IEEE Trans. Med. Imaging 17 737-42
3. Biosense Webster, a Johnson+Johnson company CARTO™ XP EP Navigation system, http://www.jnjgateway.com/home.jhtml?loc=USENG&page=viewContent&contentId=09008b98800876c3&spec=Arrhythmia_Management
4. Blood E B, “Device for quantitatively measuring the relative position and orientation of two bodies in the presence of metals utilizing direct current magnetic fields”, U.S. Patent No. 4,849,692.
5. Buchholz R D, Ho H W, Rubin J P, “Variables affecting the accuracy of stereotactic localization using computerized tomography”, Journal of Neurosurgery, 79 667-73
6. Ellsmere J, Stoll J, Wells III W, Kikinis R, Vosburgh K, Kane R, Brooks D, Rattner,D, "A New Visualization Technique for Laparoscopic Ultrasonography", Surgery, July 2004, Vol. 136, No. 1, pp. 84-92.
7. Faro Technology, Laser Tracking Interferometer, http://www.faro.com/products/Laser_Tracker_x.asp

8. Fenster A, Landry A, Downey D, Hegele R, Spence D, “3D Ultrasound Imaging of the Carotid Arteries”, Current Drug Targets – Cardiovascular & Haematological Distorders, 2004, 4 161-175
9. Ferre M R, Jakab P D, Tieman J S, “Position tracking and imaging system with error detection for use in medical applications”, U.S. Patent No. 5,676,673, 1996
10. Frantz D D, Wiles A D, Leis S E, Kirsch S R, “Accuracy assessment protocols for electromagnetic tracking systems”, Physics in Medicine and Biology, 48:2241-2251, 2003
11. Fried M, Kleefield J, Gopal H, Reardon E, Ho B, Kuhn F, “Image-guided Endoscopic Surgery: results of Accuracy and Performance in a Multicenter Clinical Study Using an Electromagnetic Tracking System”, The Laryngoscope, Vol. 107, No. 5, May 1997 pp. 594-601.
12. GE Healthcare Electromagnetic Surgical Navigation, http://www.gehealthcare.com/rad/savi/nav/home.html
13. Hummel J, Figl M, Kollmann C, Bergmann, H, Birkfellner W, “Evaluation of a miniature electromagnetic position tracker”, Medical Physics. 29 (10) 2205-2212 (October 2002)
14. Hummel J, Jun C M, Figl M, Bax M, Bergmann H, Birkfellner W, Shahidi R, “Standardized evaluation method for Electromagnetic Tracking Systems”, Medical Imaging 2005: Visualization, Image-Guided Procedures, and Display, Proc. of SPIE Vol. 5744 237-240
15. Innovmetric Polyworks Software, http://www.innovmetric.com/
16. Kuipers J, “Object tracking and orientation determination means, system and process”, U.S. Patent No. 3,868,565
17. Leotta D, "An Efficient Calibration Method for Freehand 3D Ultrasound Imaging Systems", Ultrasound in Med. & Biol., May 2004, Vol. 30, No. 7, pp. 999–1008.
18. McMASTER-CARR, Stainless Steel bar stock, http://www.mcmaster.com/
19. Medtronic Orthopaedic Navigation Solutions Brochure, http://www.stealthstation.com/files/uploads/MedtronicOrthoNavBrochure.pdf
20. Northern Digital Incorporated (NDI), http://www.ndigital.com/
21. NDI Polaris Vicra, http://www.ndigital.com/polarisvicra.php
22. NDI Aurora, http://www.ndigital.com/aurora.php
23. Polhemus, http://www.polhemus.com/
24. Raab F H, Blood E B, Steiner T O, Jones H R, “Magnetic position and orientation tracking system”, IEEE Transactions on Aerospace and Electronic Systems, 15(5), 709-718.
25. Reardon E, “Navigational Risks Associated with Sinus Surgery and the Clinical Effects of Implementing a Navigational System for Sinus Surgery”, The Laryngoscope, Vol. 112, No. 7, July 2002. pp.1-19.
26. Sagi H C, Manos R, Benz R, Ordway N R, Connolly P J, “Electromagnetic Field-Based Image-Guided Spine Surgery Part One: Results of a Cadaveric Study Evaluating Lumbar Pedicle Screw Placement, Spine”, Vol. 28, No. 17 Sept 2003. pp 2013-2018.
27. Sagi H C, Manos R, Park S C, Von Jako R, Ordway N R, Connolly P J, “Electromagnetic Field-Based Image-Guided Spine Surgery Part Two: Results of a Cadaveric Study Evaluating Thoraric Pedicle Screw Placement, Spine”, Vol. 28, No. 17 Sept 2003. pp. E351-E353.
28. Schicho K, Figl M, Donat M, Birkfellner W, Seemann R, Wagner A, Bergmann H, Ewers R, “Stability of miniature electromagnetic tracking systems”, Physics in Medicine and Biology, 50:2089-2098, 2005
29. Sztipanovits D R, Galloway R, Mawn L A, “Accuracy assessment and implementation of an electromagnetically-tracked endoscopic orbital navigation system”, Medical Imaging 2005: Visualization, Image-Guided Procedures, and Display, Proc. of SPIE Vol. 5744 648-660
30. Tru-Stone Corporation, http://www.gagesgalore.com/TruStone/Accessories_Right_Angle.htm